Ionophores and inhibition of SARS-CoV-2 ion channels

Clifford W Fong

Ionophores and inhibition of SARS-CoV-2 ion channels

Clifford W. Fong
Eigenenergy, Adelaide, South Australia, Australia.
Email: cwfong@internode.on.net

Keywords: SARS-CoV-2, Vero E6-hTMPRSS2 cells, polyether ionophores, carrier ionophores, E protein ion channel, ion channel inhibitors, voltage controlled ion channels, excitation energy, HOMO-LUMO energy gap, molecular volumes, TD DFT, quantum mechanics

Abstract

This study uses a previously described predictive quantum mechanical TD DFT method which can describe the time dependent behaviour of inhibitors of voltage controlled ion channels. The method is shown to apply to a widely diverse range of polyether antibiotic ionophores that inhibit SARS-CoV-2 infected Vero E6-hTMPRSS2 cells. The key determinants are (a) the excitation energy of the first excited state of the inhibitor, (b) the ground state HOMO-LUMO gap of the inhibitor that govern the dynamic binding between the inhibitor and the protein target, and (c) the molecular volume of the absorbed inhibitors in the virus envelope or the Vero cell membranes. The possibility that disruption of ion homeostasis caused by the antibiotics acting as carrier ionophores of metal ions such as K^+ or Ca^{++} is also explored.

Introduction

SARS-CoV-2 is an enveloped virus and similar to other coronaviruses, and is comprised of four key structural proteins: S, the spike protein, E, the envelope protein, M, the membrane protein, and N, the nucleocapsid protein. Both SARS-CoV and SARS-CoV-2 spike proteins use the angiotensin-converting enzyme 2 (ACE2) protein as a receptor for cellular entry in humans. Spike protein subunits have been widely reported as targets for vaccines, novel therapeutic antibodies, and small-molecule inhibitors.

Like SARS-CoV, SARS-CoV-2 uses the receptor angiotensin-converting enzyme 2 (ACE2) for entry and the serine protease TMPRSS2 for the virus S spike protein activation. The S protein of SARS-CoV-2 has a higher cell membrane fusion capacity compared to SARS-CoV. TMPRSS2 contains several domains: a LDL-receptor like domain, a scavenger receptor cysteine-rich (SRCR) domain and a serine protease domain. TMPRSS2 is co-expressed in human lung tissue with the ACE2 receptor. The inhibitors camostat and nafamostat have been shown to block the catalytic site of TMPRSS2. [1]

Several studies [2-4] have reviewed coronavirus proteins as ion channels and their potential as therapeutic targets. Coronavirus E proteins can also function as ion channels. Different electrophysical ion permeabilities were observed in bilayers for the E channel: the α-CoV HCoV-229 ($K^+ > Na^+ > Cl^-$) differed from the mouse hepatitis virus (β -CoV) and infectious bronchitis virus (γ -CoV) (both had $Na^+ > K^+ > Cl^-$). The electrophysiology of different ions (Na^+, K^+, Cl^-, Ca^{++} ions) on the coronavirus 3A, 4A and 8A proteins has also been discussed. Ion homeostasis in viruses has highlighted the importance of ion channel – virus interactions in viral pathogenesis. [5]

There are three viroporins encoded by the SARS-CoV-2 genome: the envelope protein E, 3A and ORF8a. Viroporins or ion channels are small and mostly hydrophobic multifunctional viral proteins that can alter cellular membranes. SARS 3A is associated with inflammasome activation as well as apoptotic and necrotic cell death. The 3A viroporin in SARS-CoV-2 was found to be a novel dimeric fold, forming a non-selective calcium (Ca^{++}) permeable cation channel. It is thought that calcium influx through 3A might be an activation trigger for calcium-dependent caspases and apoptosis, and the role of calcium permeability in 3A could be a significant therapeutic target [6]

It has been reported that SARS-CoV-2 exploits changes in metal ion concentrations to disguise itself in the body and evade immune surveillance. Varying concentrations of metal ions (positively charged atoms such as magnesium, manganese and calcium) are observed in hospitalized COVID-19 patients. [7]

It is thought that SARS-CoV-2 virion entry, host-membrane fusion and the ensuing virus replication in the host cells are governed by ion currents, ie for example Ca^{++} ions are necessary to promote viral fusion peptide insertion into the lipid bilayer and the cellular endocytosis pathway. [8]

The E protein which is the best characterized protein of SARS-CoV-2 is a small hydrophobic protein of ∼74–109 amino acids comprised of a charged cytoplasmic tail and a hydrophobic domain. This protein consists of three parts: NT (negatively charged), TMD (not recharged), and CT (negatively charged). [2-4] E protein contributes to ion channel, viroporin activity, and virus assembling. Envelope protein forms a cation-selective channel and plays a key role in the virus's ability to replicate itself and stimulate the host cell's inflammation response. The structure (determined in the closed state) of the E protein [9] is similar to an influenza protein called the M2 proton channel. Both viral proteins are made of bundles of several helical proteins. The SARS-CoV-2 E protein is very different to the ion channel proteins of influenza and HIV-1 viruses. The structure in the open state is still to be determined. Several amino acids at one end of the channel may attract positively charged ions such as calcium into the channel. It was found that amantadine, used to treat influenza and hexamethylene amiloride, used to treat high blood pressure both weakly block the entrance of the E channel. [9] Another homology study [10] has identified GLU 8 and ASN 15 in the N-terminal region were in close proximity to form H-bonds,

and two distinct “core” structures, the hydrophobic core and the central core, can regulate the opening or closing of the channel.

Cao et al [11] have modeled by molecular dynamics the pentameric SARS-CoV-2 E protein and shown it is a voltage-dependent hydrophobic channel with monovalent cation selectivity. Water molecules and monovalent cations spontaneously penetrate through the channel under a transmembrane voltage. The homology model of the pentameric structure of the SARS E protein (PDB5X29) was used for the SARS-CoV-2 E protein. Cao used a mixed lipid membrane model composed of phosphatidylcholine, phosphatidylethanolamine and phosphatidylserine to simulate the lipid environment. Leu10 and Phe19 are the hydrophobic gates that regulate ion permeability. It is thought that channel activity of the pentameric E protein is necessary for inflammasome activation and is the determinant of SARS-CoV-2 cytokine storm virulence.

Gupta et al [12] used molecular dynamics and docking studies to characterize the binding of many inhibitors to the E ion channel of the SARS-CoV-2 homology model (based on the NMR structure PDB5X29) noting that SARS-CoV and SARS-CoV-2 protein share a 94.74% sequence identity. It was found that some phytochemicals which were highly effective inhibitors reduced the random motion of the human SARS-CoV2 E protein. Also Val25 and Phe26 played a key role while interacting with effective inhibitors.

While there have been many recent reports of small molecule inhibitors that are effective against the spike protein of SARS-CoV-2, fewer studies have been made targeting the E protein ion channel. Tomar et al [13] have reported the screening of 3000 approved drugs using three independent bacteria-based assays. Ten drugs were identified with significant antiviral activity in Vero E6 tissue culture.

Voltage gated ion channels are a class of transmembrane proteins that form ion channels that are activated by changes in the electrical membrane potential near the channel. The membrane potential alters the conformation of the channel proteins, regulating their opening and closing. Cell membranes are generally impermeable to ions, thus they must diffuse through the membrane through transmembrane protein channels. Voltage gated ion channels have a particular ion selectivity and a particular voltage dependence. Many are also time-dependent in that they do not respond immediately to a voltage change but only after a delay.

Efimova 2020 [14] studied changes in the transmembrane distribution of the electrical potential by measuring changes caused by 22 alkaloids to the boundary potential of planar lipid bilayers (POPC, DOPE/DOPS or mixture of 67 mol% POPC and 33 mol% cholesterol). Membranes were also modified by the addition of pore forming anti-microbial agents GrA, SyrE, CecA, and Nys. It was found that the alkaloids had a major effect on the membrane dipole potential. The lifetime and conductance of single pores induced by the pore forming agents were also strongly

influenced by the membrane dipole potential. The tested alkaloids did not increase the ion permeability of lipid bilayers in the absence of pore-forming agents.

Broadly there are three kinds of cellular membrane potentials: the surface potentials, ($\Delta\Psi_s$), between the membrane surface and bulk solvent, resulting from the accumulation of charges at the membrane surfaces; the transmembrane potential, ($\Delta\Psi_m$), across the membrane, from one surface to the other, and determined by imbalance of charge in the aqueous solutions; and the dipole potential, ($\Delta\Psi_d$), a membrane-internal potential from the dipolar components of the phospholipids and interface water, which creates a much larger electric field that is highly localized to the interface between the hydrophobic and hydrophilic layers. The dipole potential is much larger than the surface and transmembrane potentials. The absorption of drugs into the lipophilic membrane can alter the $\Delta\Psi_d$ the membrane dipole potential by distorting the membrane and affecting conformations. $\Delta\Psi_m$ is considered to be the driving force of voltage gated ion transitions.

Efimova concluded that the dipole potential made the main contribution to the potential drop at the interface after the adsorption of alkaloids, despite some of the alkaloids having a non-zero charge at pH 7.4 based on their pKa values. The standard measures of lipophilicity, the octanol/water partition coefficient log $P_{o/w}$ (or log$D_{o/w}$ for the ionized species) were strongly correlated with the maximum dipole potential at the 0.75 level. No correlations were observed with the dipole moments of the alkaloids. [14]

Efimova 2015 [15] also similarly studied changes in the dipole potential of lipid bilayer membranes caused by the adsorption of some flavonoids, muscle relaxants, thyroid hormones, and xanthene and styrylpyridinium dyes. A quantitative relationship was found between the ratio of the maximum change in the bilayer dipole potential upon saturation and the absolute value of the unmodified membrane.

Svenningsen [16] has determined the in vitro efficacy of a wide range of polyether ionophore antibiotics against the SARS-CoV-2 infection in Vero E6-hTMPRSS2 cells. In particular the antibiotic X-206 showed displayed >500-fold selectivity and was able to inhibit viral replication even at sub-nM levels. The antiviral mechanism of the polyether ionophores is currently not understood. An earlier evaluation of a panel of 290 drugs and drug candidates against MERS-CoV and SARS-CoV, revealed that 9 different ion channel inhibitors including the polyether ionophores salinomycin and monensin could inhibit the pathogenesis effects of MERS but not SARS-CoV. [17] Zhang has noted that the ionophore valinomycin is active against coronaviruses such as SARS-CoV, MERS-CoV, human coronavirus OC43 (HCoV-OC43), and has potential to also be active against SARS-CoV-2 [18].

Study objectives:

Identify predictive methods which can describe the time dependent behaviour of polyether antibiotics possibly acting as inhibitors of voltage controlled ion channels or influencing ion homeostasis in SARS-CoV-2 infected cells

Results

Time-dependent density-functional theory (TDDFT) is a quantum mechanical theory which can describe the properties and dynamics of molecular systems in the presence of time-dependent potentials, such as electric or magnetic fields. The excitation energies of molecular systems such as the influence of chemical inhibitors on the electrical fields in voltage gated ion channels offer potential to describe such behaviour as a function of varying structural properties of such inhibitors. The time dependencies involved are (a) the dynamic inhibition equilibrium of ion channels by chemical species, (b) the electrical field imposed on the particular inhibitor-ion channel interaction.

We have previously shown [19] that the excitation energy and the ground state (HOMO-LUMO) energy gap can predicatively describe linear changes in the electrical dipole transmembrane potential of planar lipid bilayers for a wide and diverse range of flavanoids, xanthenes dyes and alkaloids. In alkaloids the lifetime and conductance of single pores induced by the pore forming agents were also strongly influenced by the membrane dipole potential. The tested alkaloids did not increase the ion permeability of lipid bilayers in the absence of pore-forming agents. We also showed that drugs which have antiviral activity by inhibiting the E protein ion channel of SARS-CoV-2 can be predicatively described by a linear dependence on the excitation energy of the drugs as well as their dynamic ground state binding to the E protein as measured by the (HOMO-LUMO) gap. [19] We have used our general LFER method [20] which seeks unconstrained linear free energy relationships amongst the vertical excitation energy of the first excited state, the ground state (HOMO-LUMO) energy gap, the lipophilicity ($\Delta G_{\mathbf{CDS},\mathrm{Octanol}}$) and the molecular volume in n-octanol (as a surrogate for the lipophilic virus coating or host cell membrane). In a study of the changes in the transmembrane distribution of the electrical potential caused by the absorption of 22 alkaloids in planar lipid bilayers, it was found that the lipophilicity, as measured by the octanol/water partition coefficient log $P_{o/w}$ (or log$D_{o/w}$ for the ionized species) was strongly correlated with the maximum dipole potential at the 0.75 level. [14]

Table 1 shows the EC_{50} values for eleven ionophore antibiotics from Svenningsen [16] and the calculated excitation energies, ground state HOMO-LUMO gaps, lipophilicities and molecular volumes in n-octanol.

Svenningsen [16] has determined the in vitro efficacy of a wide range of polyether ionophore antibiotics against the SARS-CoV-2 infection in Vero E6-hTMPRSS2 cells. For the free acid antibiotics the best correlation for EC_{50} was found for eq 1 and 2. Calculated molecular volumes have been normalized by 100 times to allow a direct comparison of the coefficients for the excitation energy and molecular volumes. Ionomycin was excluded as a demonstrated outlier from all correlations.

Eq 1 10 antibiotics (free acid form) from Svenningsen

EC_{50} = -0.09Excitation Energy – 0.11MolVol + 1.15

Where R^2 = 0.730, SEE = 0.112, SE(ExcitEn)= 0.05, SE(MolVol) = 0.03, F=9.47, Significance= 0.010. **P-values:** ExcitEn= 0.012, MolVol=0.018;

Eq 2 examines the 10 antibiotics (free acid form) from Svenningsen when tested against the HOMO-LUMO gap and the molecular volume

Eq 2 10 antibiotics (free acid form) from Svenningsen

EC_{50} = -0.095(HOMO-LUMO) – 0.11MolVol + 1.215

Where R^2 = 0.720, SEE = 0.114, SE(HOMO-LUMO)= 0.057, SE(MolVol) = 0.03, F=8.98, Significance= 0.0116. **P-values:** (HOMO-LUMO)= 0.14, MolVol=0.014;

It can be seen that eq 1 and eq 2 are very similar, suggesting that the EC_{50} values for the SARS-CoV-2 are about equally dependent on the molecular volumes of the absorbed antibiotics in the lipophilic viral envelope and the excitation energies and (HOMO-LUMO) gaps. Because of the small experimental data set for EC_{50} values, it is noted that separate linear correlations between EC_{50} and molecular volume {F 12.5, Signif 0.007}, EC_{50} and excitation energies { F 2.1, Signif 0.18}, and EC_{50} and (HOMO-LUMO) { F 3.2, Signif 0.10} were also reasonably strong correlations.

Since the antibiotics examined by Svenningsen are known ionophores it is pertinent to investigate whether the EC_{50} experimental values may be dependent on these antibiotics acting partly or substantially as carrier ionophores which can influence ion homeostasis within the virus and or Vero cells. Under the in vitro experimental conditions (Dulbecco's Modified Eagle's Medium (DMEM) and fetal calf serum, pH ~ 7.5) may provide sources of ions such as K^+, Na^+ and Ca^{++}. All of the ionophores are known to be active carriers of K^+ particularly, with A23187 calcimycin and ionmycin being active carriers of Ca^{++} ions. Examination of the antibiotics acting as ion carriers shows that the most stable forms of the {ionophore-metal ion} complexes are electrogenically neutral species where the anionic form of the antibiotic complexes with the K^+ ion in such a fashion that the antibiotic component wraps around the metal ion partially shielding the metal ion, and increasing the lipophilicity of the complexes. However $\{\text{indanomycin-}K^+\}^0$ is an exception, since it is a much smaller molecule. A23187 calcimycin requires two anionic antibiotic moieties to complex with the Ca^{++} to form a neutral complex, whereas in ionomycin the di-anionic antibiotic moiety complexes with the Ca^{++} ion to form a neutral complex.

Table 2 shows the molecular specifiers for these {antibiotic-metal} complexes in n-octanol. Figures 1 and 2 show the molecular complexes $\{X\text{-}206\text{-}K^+\}^0$ (formed from the X-206 anion and K^+) and $\{X\text{-}206\text{-}K^+\}^+$ (formed from the neutral X-206 and K^+), with lipophilicities ($\Delta G_{\mathbf{CDS},\text{Octanol}}$) of -2.74 and -3.20 kcal/mol respectively. $\{X\text{-}206\text{-}K^+\}^0$ is more stable than $\{X\text{-}206\text{-}K^+\}^+$ by 0.57 kcal/mol. Figure 3 shows $\{\text{Monensin-}K^+\}^0$ (formed from the anionic Monensin and K^+) with the intramolecular H bond, and Figure 4 showing $\{\text{Monensin-}K^+\}^+$ (formed from the neutral Monensin and K^+) *without* the intramolecular H bond and carrying a formal positive charge. It is noteworthy that $\{\text{Monensin-K}\}^0$ has a lipophilicity of -0.66 kcal/mol, while $\{\text{Monensin-K}\}^+$ has virtually the same lipophilicity of -0.71 kcal/mol. The formal positive charges on $\{X\text{-}206\text{-}K^+\}^+$ and $\{\text{Monensin-K}\}^+$ are highly delocalized. $\{\text{Monensin-}K^+\}^0$ is more stable than $\{\text{Monensin-}K^+\}^+$ by 0.82 kcal/mol. Figure 5 shows $\{\text{Ionomycin-}Ca^{++}\}^0$ with the dianionic form of ionomycin complexing with Ca^{++}, and Figure 6 shows $\{\text{dicalcimycin-}Ca^{++}\}^0$ formed by two calcimycin anions complexing with Ca^{++}.

Analysis of the EC_{50} values from Svenningsen assuming the active inhibitory species are the neutral {ionophore-metal ion} complexes (as per Table 2 shown as the K^+ complexes or otherwise as the Ca^{++} complexes for dicalcimycin and narasin) gives eq 3 and 4.

Eq 3 10 antibiotics as neutral $\{\text{ionophore-}M^{n+}\}^0$ complexes

$$\mathbf{EC_{50} = -0.089 Excitation\ Energy - 0.15 MolVol + 1.411}$$

Where R^2 = 0.612, SEE = 0.134, SE(ExcitEn)= 0.049, SE(MolVol) = 0.05, F=5.54, Significance= 0.036. **P-values**: ExcitEn= 0.114, MolVol=0.018;

Eq 4 10 antibiotics as neutral $\{\text{ionophore-}M^{n+}\}^0$ complexes

$$\mathbf{EC_{50} = -0.102(HOMO\text{-}LUMO) - 0.156 MolVol + 1.560}$$

Where R^2 = 0.667, SEE = 0.125, SE(HOMO-LUMO)= 0.044, SE(MolVol) = 0.051, F=7.03, Significance= 0.021. **P-values**: (HOMO-LUMO)= 0.061, MolVol=0.012;

It can be seen that eqs 3 and 4 are quite similar to the corresponding eqs 1 and 2, with similar precision. The strong similarities infers that the active species that inhibits the SARS-Cov-2 in Vero E6-hTMPRSS2 cells could be either the free acid form of the antibiotic ionophores or possibly the neutral $\{\text{ionophore-}M^{n+}\}^0$ complexes.

Discussion

The absorption of drugs into the lipophilic envelope of viruses or the lipophilic membrane of cells can be dependent on the molecular size of the drugs as they distort the viral envelope affecting electrical fields in voltage gated ion channels, and perturb $\Delta\Psi_d$ of the cell membrane. [14] [21] The (HOMO-LUMO) gap is a ground state property that determines the inherent chemical reactivity of the drugs and governs the dynamic equilibrium between various drugs and

the lipid membrane. The excitation energy of the first excited state is a measure of how a drug will be excited under a dynamic electrical potential.

Eqs 1 and 2 suggest that EC_{50} results for the ionophore antibiotics studied by Svenningsen indicate that ion channel inhibition of the SARS-CoV-2 virus is likely occurring, since the dependency on the excited state of the antibiotics indicates that time-dependent potentials are involved in the chemical inhibition of the electrical fields in voltage controlled ion channels. The strong dependency on the molecular volume for the adsorbed antibiotics and how they may influence the ion channel potential of the viral envelope, or the dipole potential of the cell membrane also supports this notion. Dependency on the (HOMO-LUMO) gap is consistent with the innate reactivity of the antibiotics. It is not known which ion channels or viroporins are involved in Svenningsen's study, but the envelope protein E, 3A and ORF8a are likely present. We have previously shown that the inhibition of the SARS-CoV-2 envelope protein E is determined by equations similar to eqs 1 and 2 being primarily dependent on excitation energy and the (HOMO-LUMO) gap. [19]

Eqs 3 and 4 are suggestive that since the antibiotics examined by Svenningsen are known ionophores, the EC_{50} experimental values could be dependent on these antibiotics acting partly or substantially as carrier ionophores which can influence ion homeostasis within the virus and or Vero cells. There is evidence that metal ions and accompanying disruption of ion homeostasis may be involved in the pathogenesis of Covid-19. [2,5,7,8]

The neutral $\{\text{ionophore-}M^{n+}\}^{0}$ complexes (formed from the anionic ionophore and metal ion) are shown to have similar lipophilicity and greater stability to the charged $\{\text{ionophore-}M^{n+}\}^{n+}$ (formed from the neutral ionophore and metal ion) species where the formal charge is delocalized, and accordingly are similarly likely to penetrate the lipophilic virus envelope or Vero cell membrane. The pH of the experimental DMEM medium is ~7.5 which allows some anionic ionophore to be present which can then complex with K^{+} or Ca^{++} to form the neutral $\{\text{ionophore-}M^{n+}\}^{0}$ complexes, which are stabilized by an intramolecular hydrogen bond between the anionic acid group and a hydroxyl group (see Figures 1-6)

Conclusions

This study uses a previously described predictive quantum mechanical TD DFT method which can describe the time dependent behaviour of inhibitors of voltage controlled ion channels. The method is shown to apply to a widely diverse range of polyether antibiotic ionophores that inhibit SARS-CoV-2 infected Vero E6-hTMPRSS2 cells. The key determinants are (a) the excitation energy of the first excited state of the inhibitor, (b) the ground state HOMO-LUMO gap of the inhibitor that govern the dynamic binding between the inhibitor and the protein target, and (c) the molecular volume of the absorbed inhibitors in the virus envelope or the Vero cell

membranes. The possibility that disruption of ion homeostasis caused by the antibiotics acting as carrier ionophores of metal ions such as K^+ or Ca^{++} is also explored.

Materials and methods

All calculations were carried out using the Gaussian 09 package. Energy optimizations were at the DFT/B3LYP/6-31G(d) (6d, 7f) level of theory for all atoms in water. TD DFT vertical calculations were conducted at the TD DFT/B3LYP/6-31G(d,p) (6d, 7f) with the empirical dispersion GD3BJ correction for neutral and charged compounds with optimized geometries in n-octanol, using the IEFPCM/SMD solvent model. Ground state HOMO and LUMO were calculated at the DFT/B3LYP/6-31G(d,p) (6d, 7f) with empirical dispersion GD3BJ in n-octanol.

References

[1] Hoffmann, M., Kleine-Weber, H., Schroeder, et al, SARS-CoV-2 cell entry depends on ACE2 and TMPRSS2 and is blocked by a clinically proven protease inhibitor, Cell, 2020, 181, 271–280.e8.
[2] C McClenaghan, A Hanson, SJ Lee, CG Nichols, Coronavirus Proteins as Ion Channels: Current and Potential Research, Front. Immunol., 2020, https://doi.org/10.3389/fimmu.2020.573339
[3] S Hover, B Foster, JN Barr, Jamel Mankouri, Viral dependence on cellular ion channels – an emerging antiviral target? J General Virology 2017, 98, 345–351
[4] JL Nieto-Torres, ML DeDiego, E Álvarez, et al, Subcellular location and topology of severe acute respiratory syndrome coronavirus envelope protein, Virology, 2011, 415, 69–82
[5] FW Charlton, HM Pearson, S Hover, et al, Ion Channels as Therapeutic Targets for Viral Infections: Further Discoveries and Future Perspectives, Viruses 2020, 12, 844. doi:10.3390/v1208084
[6] DM Kern, B Sorum, SS Mali, et al. Cryo-EM structure of SARS-CoV-2 ORF3a in lipid nanodiscs, Nature Structural & Molecular Biology, 2021, doi:10.1038/s41594-021-00619-0. https://www.nature.com/articles/s41594-021-00619-0
[7] T Viswanathan, A Misra, K Gupta et al, A metal ion orients SARS-CoV-2 mRNA to ensure accurate 2′-O methylation of its first nucleotide, Nature Comm, 2021, 12 (1) DOI: 10.1038/s41467-021-23594-y
[8] EP Navarese, RL Musci, L Frediani, Ion channel inhibition against COVID-19: A novel target for clinical investigation, Cardiology J, 2020, 27, 421–424
[9] VS Mandala, MJ McKay, AA Shcherbakov, et al, Structure and drug binding of the SARS-CoV-2 envelope protein transmembrane domain in lipid bilayers, Nat Struct Mol Biol, 2020, 27, 1202–1208, https://doi.org/10.1038/s41594-020-00536-8
[10] M Sarkar, S Saha, Structural insight into the role of novel SARS-CoV-2 E protein: A potential target for vaccine development and other therapeutic strategies, PLoS ONE 2020, 15(8): e0237300. https://doi.org/10.1371/journal.pone.0237300
[11] Y Cao, R Yang, W Wang, et al, Computational Study of the Ion and Water Permeation and Transport Mechanisms of the SARS-CoV-2 Pentameric E Protein Channel, Front. Mol. Biosci., 2020, https://doi.org/10.3389/fmolb.2020.565797
[12] MK Gupta, S Vemula, R Donde, et al, *In-silico* approaches to detect inhibitors of the human severe acute respiratory syndrome coronavirus envelope protein ion channel, J Biomol Struct Dynam, 2021, 39:7, 2617-2627, DOI: 10.1080/07391102.2020.1751300

[13] PPS Tomar, M Krugliak, IT Arkin, Targeted Drug Repurposing Against the SARS-CoV-2 E Channel Identifies Blockers with in vitro Antiviral Activity, bioRxiv preprint doi: https://doi.org/10.1101/2021.02.24.432490
[4] SS Efimova, AA Zakharova, OS Ostroumova, Alkaloids Modulate the Functioning of Ion Channels Produced by Antimicrobial Agents via an Influence on the Lipid Host, Front. Cell Dev. Biol. 2020, 8:537. doi: 10.3389/fcell.2020.00537
[15] SS Efimova, OS Ostroumova, Modifiers of the dipole potential of lipid bilayers, Acta Nat. 2015, 7, 70-79. doi: 10.32607/20758251-2015-7-4-70-79
[16] EB Svenningsen, J Thyrsted, J Blay-Cadanet, et al, Ionophore antibiotic X-206 is a potent inhibitor of SARS-CoV-2 infection *in vitro*, Antiviral Res, 2021, 185, 104988
[17] J Dyall, CM Coleman, BJ Hart, et al, Repurposing of clinically developed drugs for treatment of Middle East respiratory syndrome coronavirus infection, Antimicrob. Agents Chemother. 2014, 58, 4885–4893
[18] D Zhang, Z Ma, H Chen, Y Lu, X Chen, Valinomycin as a potential antiviral agent against coronaviruses: A review, 2020, Biomed J. 43, 414–42
[19] CW Fong, Inhibition of SARS-CoV-2 envelope ion channel and the relationship with the membrane dipole potential, hal archives, 2021, https://hal.archives-ouvertes.fr/hal-03200926
[20] CW Fong, COVID-19: Predicting inhibition of repurposed drugs for SARS-CoV-2 viral activity and cellular entry**,** hal archives 2020, hal-02963306v1
[21] LJ Mares, A Garcia, HH Rasmussen, RJ Clark, Identification of Electric-Field-Dependent Steps in the Na^+, K^+ - Pump Cycle, Biophys J. 2014, 107, 1352-1363

Table 1. Molecular specifiers for free acid form of ionophores: EC_{50} inhibition of SARS-CoV-2 infected Vero E6-hTMPRSS2 cells from ref 16

Free acid Ionophores	Excitation Energy eV	(HOMO-LUMO) eV	$\Delta G_{CDS,Octanol}$ kcal/mol	Molecular Volume cm^3/mol	EC_{50} µM
Nigericin	4.641	4.984	0.54	472	0.09
Monensin	5.154	5.703	-1.26	465	0.1
Salinomycin	4.132	5.737	-1.98	518	0.1
Indanomycin	3.45	4.179	-1.78	328	0.63
Lasalocid	4.251	5.34	-1.7	439	0.36
A23187 Calcimycin	3.491	4.02	0.96	440	0.26
Narasin	3.698	5.039	-1.76	577	0.07
Nanchangmycin	3.659	4.861	0.09	673	0.07
Maduramycin	3.854	4.647	2.28	724	0.06
X-206	5.638	6.195	-1.81	643	0.014
Ionomycin	3.849	4.898	-0.81	633	3

Table 2. Molecular specifiers for {ionophore-M^{n+}}^{0} complexes: EC_{50} inhibition of SARS-CoV-2 infected Vero E6-hTMPRSS2 cells from ref 16

{Ionophore-M^{n+}}^{0} Complexes	Excitation Energy eV	(HOMO-LUMO) eV	$\Delta G_{CDS,Octanol}$ kcal/mol	Molecular Volume cm^3/mol	EC_{50} µM
{Nigericin-K}(0)	4.65	5.052	-0.85	609	0.09
{Monensin-K}(0)	5.429	6.4	-0.66	528	0.1
{Salinomycin-K}(0)	3.974	4.577	-1.32	525	0.1
{Indanomycin-K}(0)	3.488	4.185	-2.12	380	0.63
{Lasalocid-K}(0)	4.105	4.609	-1.25	559	0.36
{Dicalcimycin-Ca}(0)	2.803	3.226	1.6	705	0.26
{Narasin-K}(0)	3.974	4.550	-1.41	592	0.07
{Nanchangmycin-K}(0)	3.858	4.775	-0.18	673	0.07
{Maduramycin-K}(0)	2.575	3.605	1.54	634	0.06
{X-206-K}(0)	5.202	5.696	-2.74	634	0.014
{Ionomycin-Ca}(0)	4.035	4.989	-2.47	533	3

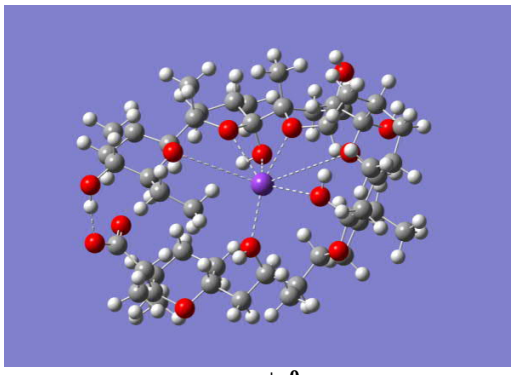

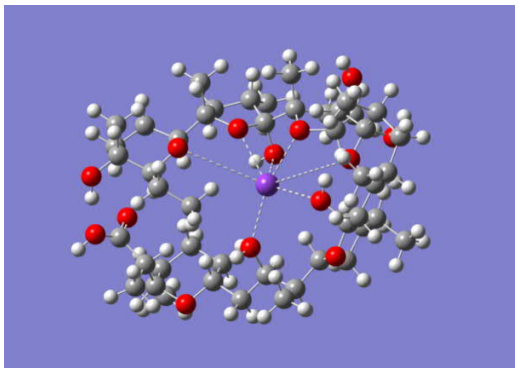

Fig 1(left) {X-206-K^+}^{0} showing intramolecular H bond left edge & Fig 2(right) {X-206-K^+}$^+$ *without* the intramolecular H bond

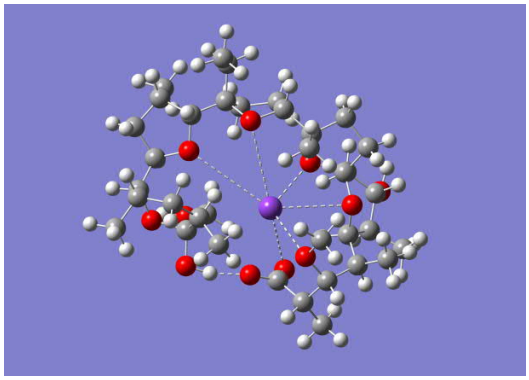

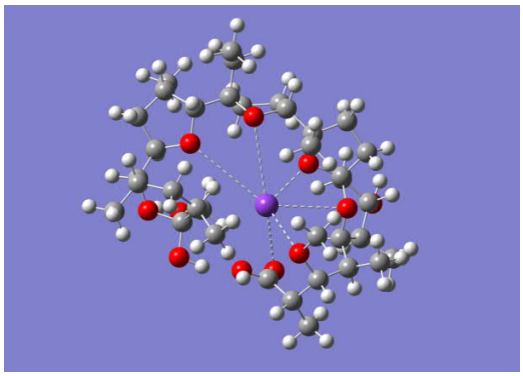

Fig 3(left) {Monensin-K^+}^{0} showing intramolecular H bond bottom edge, and Fig 4(right) showing {Monensin-K^+}$^+$ *without* intramolecular H bond bottom edge

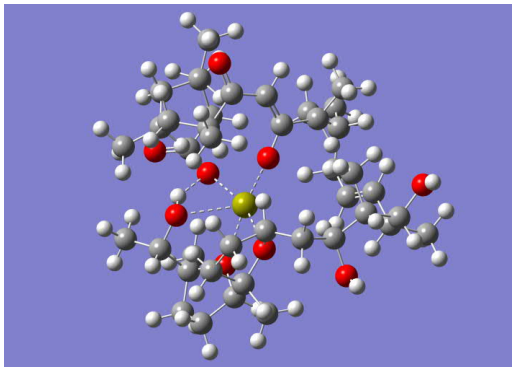

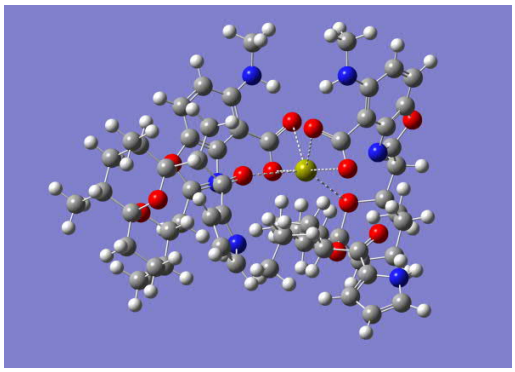

Fig 5 (left) {Ionomycin-Ca^{++}}^{0} showing dianionic form of Ionomycin complexing with Ca^{++} and Fig 6 (right) showing {Dicalcinycin-Ca^{++}}^{0} with 2 calcimycin anions complexed to Ca^{++}